Inkjet-Printed PEDOT:PSS-based Stretchable Conductor for Wearable Health Monitoring Device Applications

Li-Wei Lo,[†,§] Junyi Zhao,[†] Haochuan Wan,[†] Yong Wang,[†,‡] Shantanu Chakrabartty,[†] and Chuan Wang[,†,§]*

[†] Department of Electrical & Systems Engineering, Washington University in St. Louis, St. Louis, Missouri 63130, United States

[§] Institute of Materials Science and Engineering, Washington University in St. Louis, St. Louis, Missouri 63130, United States

[‡] Department of Obstetrics & Gynecology, Washington University in St. Louis, St. Louis, Missouri 63130, United States

[*] Corresponding author: chuanwang@wustl.edu

ABSTRACT

Stretchable conductor is one of the key components in soft electronics that allows seamless integration of electronic devices and sensors on elastic substrates. Its unique advantages of mechanical flexibility and stretchability have enabled a variety of wearable bioelectronic devices that can conformably adapt to curved skin surface for long-term health monitoring applications. Here, we report a poly(3,4-ethylenedioxythiophene) polystyrene sulfonate (PEDOT:PSS)-based stretchable polymer blend that can be patterned using an inkjet printing process while exhibiting low sheet resistance and accommodating large mechanical deformations. We have systematically studied the effect of various types of polar solvent additives that can help induce phase separation of PEDOT and PSS grains and changes the conformation of PEDOT chain thereby improving the electrical property of the film by facilitating charge hopping along the percolating PEDOT network. The optimal ink formulation is achieved by adding 5 wt% of ethylene glycol into pristine PEDOT:PSS aqueous solution which results in a sheet resistance of as low as 58 Ω/□. Elasticity can also be achieved by blending the above solution with soft polymer poly(ethylene oxide) (PEO). Thin-films of PEDOT:PSS/PEO polymer blends patterned by inkjet printing exhibits low sheet

resistance of 84 Ω/□ and can resist up to 50% of tensile strain with minimal changes in electrical performance. With its good conductivity and elasticity, we have further demonstrated the use of the polymer blend as stretchable interconnects and stretchable dry electrodes on thin polydimethylsiloxane (PDMS) substrate for photoplethysmography (PPG) and electrocardiography (ECG) recording applications. This work shows the potential of using printed stretchable conducting polymer in low-cost wearable sensor patch for smart health applications.

KEYWORDS: printed electronics; stretchable electronics; conductive polymer; wearable sensors; health monitoring devices

INTRODUCTION

Over the past decade, flexible electronics such as displays, solar cells, and various types of sensors that can retain their performance and functionality while being bent have been explored extensively.[1–7] Flexible sensors for continuous vital sign monitoring and other health care application have also been developed but these devices are not ideal because the human skin surface is not only flexible but also soft and stretchable.[8–12] Without being able to form intimate contact and conformably adapt to human skin, the sensors may detach or slide on the skin resulting in motion artifact and inaccurate or fluctuating readings. In order to achieve wearable sensors with more stable signal recording and better wearing comfort, soft electronic devices that are stretchable and have the ability to accommodate large strain and deformations while maintaining their electrical performance have attract significant attention. Progress has been made in demonstrating soft electronics for applications in artificial electronic skin, soft robotics and wearable sensors.[13–20]

Stretchable conductor is one of the key components for implementing soft electronics and there are a few approaches to achieve stretchable conductors. The first is to use conventional metal thin films but pattern them into buckling, wavy or serpentine shaped patterns that are structurally-stretchable.[21–23] This approach utilizes conventional microfabrication processes that are highly reliable and typically results in great electrical performance although the sample is sometimes limited to small or medium sizes due to the constraints in microfabrication tools. The second approach is to develop intrinsically-stretchable composite materials by adding conductive fillers such as carbon nanotubes (CNT),[24,25] metal nanoparticles or metal nanowires[26–29] into elastomers such as polydimethylsiloxane (PDMS). Such composite materials generally offer good stretchability but the use of insulating polymer matrix could result in either low conductivity or significant conductivity change under mechanical deformation. An alternative method for achieving intrinsically-stretchable polymer is to blend soft polymer or plasticizer into conducting polymers that may soften the polymer chain and thus increase the free volume resulting a low modulus material. For example, it has been reported that the widely used conducting polymer poly(3,4-ethylenedioxythiophene) polystyrene

sulfonate (PEDOT:PSS) can be made stretchable by blending in poly(ethylene glycol) (PEG), poly(vinyl alcohol) (PVA), polyurethane (PU) or Zonyl.[30–36] Such polymer blends are solution processable and can be made into large area conductive thin films for stretchable electrode applications using low-cost processes such as spin coating.[30,33]

In order to achieve high resolution patterning of the solution-based stretchable conducting polymer, printing methods such as inkjet printing can be used.[37–41] However, one challenge is that most of the soft polymer additives with high molecular weights are often too viscous. In order to make the ink suitable for inkjet printing, the viscosity needs to be lowered and its surface tension needs to be adjusted for optimal wetting on elastomer substrates. The above can be achieved by diluting the polymer with appropriate organic solvents.[42,43] In this work, we have systematically studied the effect of adding polar solvents on the most commonly use water-soluble conducting polymer PEDOT:PSS, where PEDOT with positive charges and insulating PSS with negative charges that stabilized PEDOT configuration by columbic attractions.[44] The electrical properties of PEDOT:PSS and have found that the best conductivity can be achieved by adding ~ 5 wt% of ethylene glycol (EG).

To achieve stretchability, we have formulated an ink recipe by dissolving polymer poly(ethylene oxide) (PEO) in N,N-Dimethylformamide (DMF) to reduce its viscosity and then mixing with PEDOT:PSS solution that can decrease the interaction between polymer chains and increase the free volume between PEDOT and PSS grains to make a highly stretchable ink with low sheet resistance[16]. After patterned using inkjet printing, thin films of intrinsically-stretchable PEDOT:PSS/PEO polymer blend exhibits a low sheet resistance of 84 Ω/□ and a high stretchability of up to 50%. In addition to its high stretchability and conductivity, the PEDOT:PSS/PEO polymer blend is also biocompatible and can be made into wearable sensor patches for health monitoring applications.[45–48] As an example, we have demonstrated an inkjet-printed sensor patch on PDMS substrate for recording vital signs including electrocardiography (ECG) and photoplethysmography (PPG). Unlike traditional Ag/AgCl electrodes with conducting hydrogel between skin and electrodes, the printed PEDOT:PSS/PEO polymer blend is not only stretchable but can also be

used as dry electrodes that can be directly placed on skin surface without the use of conducting hydrogel. In the PPG monitoring application, the printed PEDOT:PSS/PEO is used as stretchable interconnects for connecting a surface-mount light-emitting diode and a photodetector. The printed sensor patch can simultaneously and continuously record ECG and PPG waveforms for monitoring the heart rate, blood oxygen and cardiac cycles. It serves as a proof-of-concept demonstration to show the potential of using printed stretchable conducting polymer in low-cost wearable sensor patch for smart health applications.

RESULTS AND DISCUSSION

The chemical structure of the conducting polymer PEDOT:PSS, the polar solvent EG, dimethyl sulfoxide (DMSO), DMF, glycerol and the soft PEO are shown in Figure 1a. PEDOT is the most widely used conducting polymer in the past decade due to its high conductivity, transparency and stability. The most commonly used commercially available product of PEDOT comes with PEDOT doped with PSS. This aqueous dispersion consisting PEDOT-rich particles surrounded by PSS-rich shells, with the negatively charged polyanion (PSS^-) stabilizing the positively charged polycation ($PEDOT^+$). The polyanion (PSS^-) is an insulator that hampers the charge transport pathway through polycation ($PEDOT^+$) and results in low electrical conductivity of less than 1 S cm^{-1} in pristine PEDOT:PSS. One of the solutions to improve its conductivity is by adding polar solvents into the pristine PEDOT:PSS aqueous solution to achieve phase separation between PEDOT and PSS grains and the conformational change of the PEDOT chain. [49,50] The detail mechanism and experimental results will be discussed later. Despite the increase of conductivity after the addition of polar solvent, the mechanical properties of PEDOT:PSS thin film is too brittle to resist any large deformations. In order to address the challenge, here we report a method to achieve printable and stretchable conducting polymer by blending soft polymer poly (ethylene oxide) (PEO) and EG solvent with PEDOT:PSS. The rearranged microstructure of rigid PEDOT grains and soft PSS/PEO domains would remove the brittleness of PEDOT:PSS and yield a stretchable PEDOT:PSS/PEO polymer blend. As schematically illustrated in Figure 1b, such polymer ink can be formulated to appropriate viscosity to allow it to be directly patterned using inkjet printing process. In order to facilitate the wetting of the ink on

hydrophobic surfaces such as PDMS, the elastomeric substrate can be pretreated with oxygen plasma. After treatment, the PEDOT:PSS/PEO composite ink can be patterned onto the pretreated PDMS substrate with feature size as small as 400 μm. More details about the ink formulation and printing process can be found in the experimental section. Figure 1c shows a sample with the composite PEDOT:PSS/PEO ink printed on a 0.5 mm thick PDMS substrate. The composite polymer thin film exhibits high stretchability without any crack formation after multiple stretching cycles with tensile strain up to 50%.

While the polar solvent additives can address the low conductivity of pristine PEDOT:PSS, the number of printing passes and consequently the film thickness also play an important role in both the optical and electrical properties of the printed PEDOT:PSS thin film. As shown in Figure 2, we have systematically studied the effect of printing passes on the film thickness and the sheet resistance of the printed thin films with various types of solvent additives. The cross-sectional scanning electron microscope (SEM) images taken from the inkjet-printed PEDOT:PSS thin films with 5 wt% EG are shown in Figure 2a. With 1, 5, 10, and 20 printing process, the printed PEDOT:PSS film thickness increases monotonically, which also causes the transparency of the PEDOT:PSS thin film to decrease as shown in Figure 2b. The relationship between the film thickness with respect to the printing passes is presented in Figure 2c. The thickness of a single printing pass, 5, 10 and 20 printing passes are measured to be 0.51, 1.68, 2.84 and 3.9 μm, respectively. The corresponding UV-Vis spectra of inkjet-printed PEDOT:PSS thin film is presented in Supporting Information Figures S1.

In order to determine the best polar solvent additive, we have systematically studied the electrical properties of printed PEDOT:PSS thin films with EG, DMSO, DMF and glycerol. 5 wt% of each polar solvent was mixed into separate surfactant-free PEDOT:PSS aqueous solution (1.1% in H_2O, surfactant-free, high-conductivity grade). Additionally, 1 wt% of Triton-X was also added into the solution to tune its surface energy for optimal inkjet printing results. After printing, the film was placed on a hotplate and annealed at 120 °C for 15 min. The comparison of sheet resistance for various solvent additives with different numbers of printing passes are shown in Figure 2d. As expected, the data from the solvent-free PEDOT:PSS aqueous

ink exhibits the highest sheet resistance of ~ 6.2 kΩ/□ with a single pass printing. Other films with polar solvent additives show significantly lower sheet resistance, with 5 wt% EG exhibiting the lowest sheet resistance of ~ 355 Ω/□. The samples with 5 wt% of DMSO, 5wt% of DMF, and 5 wt% of glycerol exhibit sheet resistance of 767 Ω/□, 1914 Ω/□, and 2371 Ω/□, respectively. The results above indicate that polar solvents are indeed effective in improving the electrical property of the PEDOT:PSS. In order to reach even lower sheet resistance, the number of printing passes can be increased. With 20 passes, the sample with 5 wt% EG additive exhibits the lowest sheet resistance of 58 Ω/□ and the one with 5 wt% DMSO exhibits the second lowest sheet resistance of 72 Ω/□. Furthermore, according to Figure 2d, both EG and DMSO additives are effective in lowering the sheet resistance of PEDOT:PSS. In order to have a better understanding on both additives and find the optimal ink composition, we have also compared the sheet resistance of PEDOT:PSS inks with different amount of solvent additives ranging from 0 wt% to 10 wt% as shown in Figure 2e. The results show that the PEDOT:PSS thin films with 1 wt% DMSO exhibits slightly lower sheet resistance of 61 Ω/□ compared to 68 Ω/□ from the sample with 1 wt% EG. As the solvent content increases to 10 wt%, samples with both types of additives show inferior performance compared to 1wt% and 5 wt%. The optimal ink formulation for DMSO and EG were obtained at 1 wt% and 5 wt%, respectively. However, because the one with 5 wt% of EG exhibits the lowest sheet resistance among all experimental conditions, we have chosen this as the optimal ink formulation for further experiments.

The decrease in sheet resistance in printed PEDOT:PSS thin film with EG additive can be attributed to the morphology change of the PEDOT and PSS grains. High resolution topography and phase images of the surface of the printed PEDOT:PSS thin films were obtained using atomic force microscopy (AFM) are shown in Figure 3a and 3b. It has been reported that PEDOT and PSS grains can be differentiated by using AFM phase images,[51] where the dark regions correspond to soft materials and the bright regions correspond to more rigid polymers. In PEDOT:PSS thin film, PSS is considered as a softer polymer and PEDOT is considered to be more rigid.[35] Figure 3a shows the height image of pristine PEDOT:PSS thin film with a root-mean-square roughness of 1.7 nm and the phase image indicates that small PEDOT grains are

surrounded by small PSS grains. These insulating PSS grains hinder the carrier transport and impede the charge hopping with a discontinuous conducting pathway of PEDOT that results in a less conductive film. With the addition of EG, the PEDOT and PSS grains rearrange with thermal annealing, which separates the PEDOT grains from PSS grains as shown in Figure 3b. The microstructure of the thin film is more percolated due to the aggregation of the PEDOT grains (brighter region in the phase image) and this percolating network could aid the charge hopping along the chain that leads to a more conductive film. The effect of the aforementioned morphology change with the help of polar solvent is schematically illustrated in Figure 3c and 3d.

Although the thin film of PEDOT:PSS with EG additive exhibits superior sheet resistance, the film is still unable to resist any significant deformation. When a large tensile strain (greater than 25%) is applied, the sheet resistance of the film will increase over 250% due to the formation and propagation of microcracks. In order to make the conducting polymer stretchable, one possible way is to add soft polymer blends or plasticizers to decrease the interaction between polymer chains and increase the free volume between PEDOT and PSS grains.[52] Previous literatures have shown that by adding soft polymer such as PEG, PVA, PDMS or PU into PEDOT:PSS to form polymer blends can effectively decrease the Young's modulus and increase the elongation at break (Supporting Information Table S1).[30,31,33,53,54] While this approach could result in the desired elasticity, the PEDOT:PSS polymer blends may also experience a decrease in electrical conductivity due to the insulation of these soft polymers. Moreover, some soft polymers such as PDMS are intrinsically hydrophobic, which may be difficult to mix uniformly in the aqueous PEDOT:PSS solution and its high viscosity also makes it challenging to fabricate high resolution patterns through inkjet printing. In this work, we have selected a water-soluble soft polymer PEO as the polymer filler that can effectively encompass the brittle PEDOT and soft PSS grains.[55] In addition to making the PEDOT:PSS film stretchable, PEO can also facilitate the phase separation of PEDOT and PSS grains to form a more conductive network of PEDOT grains, which can offset the decrease in electrical conductivity due to the addition of insulating fillers. Unlike the solvent additives described above, PEO remains in the printed PEDOT:PSS thin film

even after annealing at elevated temperatures. The hydroxyl groups on PEO may form strong hydrogen bonds with the sulfonic groups on PSS, thereby weakening the interaction between PEDOT and PSS chain and thus forming a more connective PEDOT network.[56] As a result, adding PEO into PEDOT:PSS and EG can result in highly stretchable thin films while maintaining its electrical performance.

We have compared the structure change of thin films of PEDOT:PSS with EG additive before and after adding PEO. The thin films were inkjet-printed onto PDMS substrate followed by thermal annealing at 120 °C for 15 min and the samples were then mounted on a linear stage for stretch test. Figure 4a show the optical micrographs of printed thin films of PEDOT:PSS with 5 wt% EG in its relaxed state (left) and when being stretched to 50% (right). Under 50% of tensile strain, the formation of microcracks can be easily seen from the images, which greatly affects the electrical properties of the film. In contrast, according to Figure 4b, similar printed thin films of PEDOT:PSS with 5 wt% EG and 66 wt% of PEO additive show only minor cracks at the edges of the pattern under the same amount of strain. The SEM image of PEDOT:PSS thin film with 5 wt% EG and 66 wt% of PEO is presented in Figure 4c. The image shows the incorporation of crystalline PEO within the PEDOT:PSS thin film. Moreover, AFM images in Figure 4d show larger bright regions compared with the phase image in Figure 3b which indicates the PEDOT grains and the dark regions are soft PEO and PSS. The incorporation of PEO in PEDOT forms a percolation network as expected, which aids the charge transport similar to the effect of polar solvents. However, the decrease in PEDOT concentration and increase in PEO content can also negatively affect the electrical property of the PEDOT:PSS/PEO polymer blend. Figure 4e shows the sheet resistance of the film with various amount of PEO. Before adding PEO, the sheet resistance of the PEDOT:PSS thin film with 5 wt% EG is ~ 58 Ω/□. With 50 wt% (1:1) or 66 wt% (1:2) of PEO added, the sheet resistance increases to ~ 84 Ω/□ and 205 Ω/□, respectively. More details of the stability of inkjet-printed PEDOT:PSS thin film over time is presented in Supporting Information Figures S2. The results are expected due to lower percentage of PEDOT presented in the solution and the presence of insulated PEO.

Beside the effect of PEO additive on sheet resistance, the change in electromechanical property is also examined through stretch tests and the results are presented in Figure 4f. 0.5-mm-thick PDMS substrates with printed PEDOT:PSS or PEDOT:PSS/PEO thin films were mounted on a linear stage and liquid metal (EGaIn) droplets were placed on both ends of the films for measurement purpose. The electrical measurements were performed after the fresh samples were first stretched for 20 cycles. The PEDOT:PSS sample without PEO exhibits poor mechanical property with the sheet resistance increases by 20% ($\Delta R/R_0$ = 0.2, where ΔR is the change in sheet resistance and R_0 is the sheet resistance in relaxed state) when the film is stretched by 10%. Moreover, the sheet resistance increases dramatically by 250% ($\Delta R/R_0$ = 2.5) under 25% of tensile strain. In contrast, for the samples with 50 wt% or 66 wt% PEO additives, under 10% of tensile strain, the sheet resistance increases by only 9% or 1%, respectively. As the tensile strain increases to 50%, the sample with 50 wt% of PEO additive experienced 41% increase in sheet resistance while the one with 66 wt% of PEO additives only rise by 18%. We have also studied the electrical properties of PEDOT:PSS/PEO thin film when stretched in transverse direction and the data is presented in Supporting Information Figure S3. The results clearly show that the PEO additive is very effective in rendering the PEDOT:PSS film stretchable. The stability of the PEDOT:PSS/PEO polymer blend under cyclic stretch tests were also studied and the results are presented in Figure 4g. The samples with PEDOT:PSS/PEO polymer blend was repeatedly stretched to 50% of tensile strain for 1000 cycles and $\Delta R/R_0$ remained almost unchanged at 20% or 42% for the samples with 50 wt% or 66 wt% of PEO, respectively.

In both ink formulations, the PEDOT:PSS/PEO polymer blends show good stability and compliance to mechanical strain without significant sacrifice in electrical performance. Although the ink with 66% of PEO offers the best stretchability, the sheet resistance is also much higher compared to the one with 50% of PEO. For wearable electronics applications, human skin surface normally experiences no more than 30% of tensile strain.[57] As a result, it is a good tradeoff to choose the formulation with 50 wt% of PEO additive.

The above PEDOT:PSS/PEO composite ink can be processed into intrinsically-stretchable electrodes or conductors for wearable electronics and bioelectronic applications. In Figure 5, we have demonstrated an

inkjet-printed PEDOT:PSS based soft sensor patch for electrocardiography (ECG) and photoplethysmography (PPG) recording, allowing users to track the cardiac activity, cardiac cycle and heart rate simultaneously. The schematic and photograph of the prototype of the integrated soft sensor patch are shown in Figure 5a and Figure 5b. As an exemplary use case, the user may attach the sensor patch on its right wrist where one of the printed PEDOT:PSS/PEO electrodes on the backside of the PDMS substrate is in close contact with the skin. One finger from the left hand can then be placed on top of another ECG electrode on the front side of the PDMS substrate and the other finger placed on the PPG sensor comprising a red light-emitting diode (LED) and a photodiode (PD) (Figure 5c). Demonstration of the PPG recording is represented in Figure 5d-f, where the printed PEDOT:PSS/PEO film servs as stretchable interconnects between rigid circuit components (surface-mount LED and PD). The PPG sensor can be used in both reflectance and transmission modes (Figure 5f). In the reflectance mode, the red LED and the PD are placed on the same side of the finger. Due to the fact that blood absorbs more light than surrounding tissue, the small variations in the volume change between systolic and diastolic phase can be observed by the intensity change of backscattered light reaching to the photodiode.[58] In addition to reflectance mode, the soft sensor patch can also be wrapped around the fingertip and transformed into a transmission mode PPG. The red LED is now located at the fingernail whereas the PD is placed at the bottom of the fingertip. The photodiode then detects the intensity of the transmitted light through the tissue and blood vessel. Both modes of the PPG recordings provided valuable signals of the heart rate and the cardiovascular system activity. Both modes of PPG waveforms were recorded and presented in Figure 5d and e. The waveforms show clear periodic peaks that correspond to a heart rate of 72 bpm.

The printed stretchable PEDOT:PSS/PEO polymer blend can also be used as dry electrodes for ECG recording applications and the results are presented in Figure 5g-i. The PEDOT:PSS/PEO electrodes were inkjet-printed on both sides of the PDMS substrate with one electrode attached on the user's wrist and another attach to the finger while a third electrode is placed on the user's thigh and served as a ground electrode. The three electrodes were connected to a commercial ECG monitor IC (AD8232, SparkFun) for

data recording. To illustrate that the soft sensor patch can conformably adapt to the skin and the stretchability of the electrodes, two sets of ECG measurements were performed with wrist flat and bent. Both waveforms in Figure 5g are periodic and represent the phases of electrical activity of the heartbeat. The two waveforms closely resemble each other, which demonstrates the stretchability of the PEDOT:PSS electrodes without mechanical or electrical failure under applied strain in a bent wrist. In Figure 5h, the recorded ECG waveforms exhibit clearly distinguishable QRS interval and T waves, in which the QRS complex represents ventricular depolarization and the T waves reflect the ventricular repolarization.[59] These signals can be further used to detect cardiovascular diseases, such as arrhythmias and myocardial infarction.[60,61]

CONCLUSION

In Summary, we have developed an inkjet-printable and stretchable PEDOT:PSS/PEO polymer blend with PEO to help improve elasticity and polar solvent to help improve electrical conductivity and tune the ink rheology. Using the optimal ink formulation and printing recipe, printed thin films with a low sheet resistance of 84 Ω/□ that can resist up to 50% of tensile strain for thousands of cycles has been achieved. We have further demonstrated that the stretchable polymer blends can be used as printed interconnects and electrodes to form an ultrathin wearable sensor patch for PPG and ECG monitoring applications. In particular, PPG was demonstrated in both reflectance and transmission mode and the recorded signal clearly shows the pulsatile of blood in the tissue with indication of periodic systolic and diastolic peaks. The ECG waveforms collected from the polymer electrodes represents the activity of the ventricular during different phase of heart beats. The highly elastic conductive material and lightweight soft sensor patch developed in this work may lead to low-cost wearables for vital sign and cardiovascular disease monitoring and various other smart connected health applications.

METHODS

Materials

Poly(3,4-ethylenedioxythiophene)-poly(styrenesulfonate) (1.1% in H_2O, surfactant-free, high-conductivity grade), ethylene glycol (EG) (anhydrous, 99.8%), dimethyl sulfoxide (DMSO) (anhydrous, ≥99.9%), N,N-Dimethylformamide (DMF) (anhydrous, 99.8%), glycerol (99.5%), poly(ethylene oxide) (PEO) (powder, average M_v ~ 5,000,000), Triton-X 100 (laboratory grade) were purchased from Sigma-Aldrich, Eutectic gallium-indium (EGaIn) was purchased from RotoMetals and silver conductive epoxy was purchased from MG Chemicals. Polydimethylsiloxane (PDMS) (Sylgard 184) was purchased from Dow Corning.

Preparation of PEDOT:PSS/PEO ink solution

Polar solvent (EG, DMSO, DMF and glycerol) from 1 wt%, 5 wt% or 10 wt% incorporated with 1 wt% of Triton-X 100 as surfactant were added into surfactant-free PEDOT:PSS aqueous solution. The prepared solution was then stirred at room temperature for 2 h. PEO was first dissolved in DMF to give a concentration of 10 mg/mL. Afterwards, 5 wt% of ethylene glycol, 1 wt% of Triton-X 100 and the desired weight ratio of PEO solution were then added into the surfactant-free PEDOT:PSS aqueous solution. The solution was then stirred at room temperature for 3 h. The weight fraction of each solvent or additives was calculated from the additive weight divided by the total weight of the solution.

Preparation of PDMS substrate

The PDMS substrate was prepared by mixing the PDMS prepolymer with the curing agent with a mixing ratio of 10:1 w/w. Two Rain-X (ITW Global Brands) pretreated glass slides with a dimension of 1.5 in. x 1 in. and a 0.5 mm spacer were then used to cast a 0.5 mm thick PDMS substrate. Vacuum desiccator was used to eliminate the bubbles from the film and the sample was subsequently cured at 80 °C for 3 h.

Inkjet printing of PEDOT:PSS thin film on PDMS

The PDMS substrate was pretreated by oxygen plasma at 30 W for 15 s. The as prepared PEDOT:PSS or PEDOT:PSS/PEO solution were then printed onto the treated PDMS substrate using a GIX Microplotter (Sonoplot Inc.) with nozzle openings of 50-200 μm. After printing, the samples were placed on a hotplate and annealed at 120 °C for 15 min. Due to the high boiling point of glycerol, the sample of PEDOT:PSS with 5 wt% glycerol additive was annealed at 150 °C for 60 min. To investigate the printability and optimize the printing results, we have systematically studied the rheological properties and surface tension of various ink formulations and the results are shown in Supporting Information Figure S4 and Table S2.

Characterization of the printed PEDOT:PSS thin films

The width (*W*) and the length (*L*) of the inkjet-printed PEDOT:PSS thin films were measured by optical microscope (Olympus BX53M). A Semiconductor Device Analyzer (Keysight B1500A) was used to measure the electrical resistance (*R*) of the printed feature. The sheet resistance (R_s) was calculated with $R_s = R/(L/W)$. The thickness and the microstructure of the thin films were measured and captured by the environmental scanning electron microscope (Thermofisher Quattro S ESEM) and atomic force microscope (Bruker Dimensions ICO AFM). The cyclic stretching test of the thin films were performed on a modified syringe pump with 3D-printed clamps. Eutectic gallium-indium (EGaIn) was placed on both end of the thin film and connected with copper wires to the Semiconductor Device Analyzer (Keysight B1500A) to acquire the sheet resistance (R_s).

Fabrication and Characterization of the sensor patch with ECG and PPG sensors

The stretchable conductors were prepared using the PEDOT:PSS/PEO solution containing 50 wt% of as prepared PEO solution (10 mg/mL), 5 wt% ethylene glycol and 1 wt% Triton-X 100. The solution was then inkjet-printed onto a 0.5-mm-thick PDMS substrate pretreated by oxygen plasma (30 W for 15 s) followed by annealing at 120 °C for 15 min. A 3D-printed plastic stencil mask was used for patterning conductive silver epoxy as the binder between stretchable PEDOT:PSS/PEO conductors and other electronic components including light-emitting diode, photodiode and copper wires. The electrocardiogram was

captured by placing three separate PEDOT:PSS/PEO electrodes on human body (wrist, finger and thigh) and connected to a commercial heart rate monitor IC (AD8232, SparkFun). The photoplethysmography was achieved by pairing a red light-emitting diode (625 nm, XPEBRD-L1-0000-00501, Cree Inc.) and a photodiode (PDB-C152SMCT-ND, Advanced Photonix). A 5 V reverse bias was applied to the photodiode and the photocurrent was recorded using a Semiconductor Device Analyzer (Keysight B1500A). The experiment involving human subject has been performed with the full, informed consent of the volunteer, who is also the first author of the manuscript.

Supporting Information

The Supporting Information is available free of charge on the ACS Publications website at

UV-Vis spectra of inkjet-printed PEDOT:PSS thin film (S1); Electrical characterization of the printed PEDOT:PSS/PEO thin film over time (S2); Electrical Properties of PEDOT:PSS/PEO thin film when stretched along the transverse direction (S3); Rheological properties of the PEDOT:PSS-based conducting polymer ink (S4); Comparison of PEDOT:PSS based conductor with various kinds of treatment and fabrication methods (Table S1); Summary of ink formulations and measured properties (Table S2).

Conflict of Interest

The authors declare no competing financial interests.

Acknowledgements

This work was partially funded by a Washington University Collaboration Initiation Grant (CIG) and a Bill & Melinda Gates Foundation Grant (INV-005417). The authors acknowledge the

Institute of Materials Science and Engineering at Washington University for the use of instruments and staff assistance and Professor Patricia Weisensee's group for help with the ink surface tension measurement.

Figure 1.

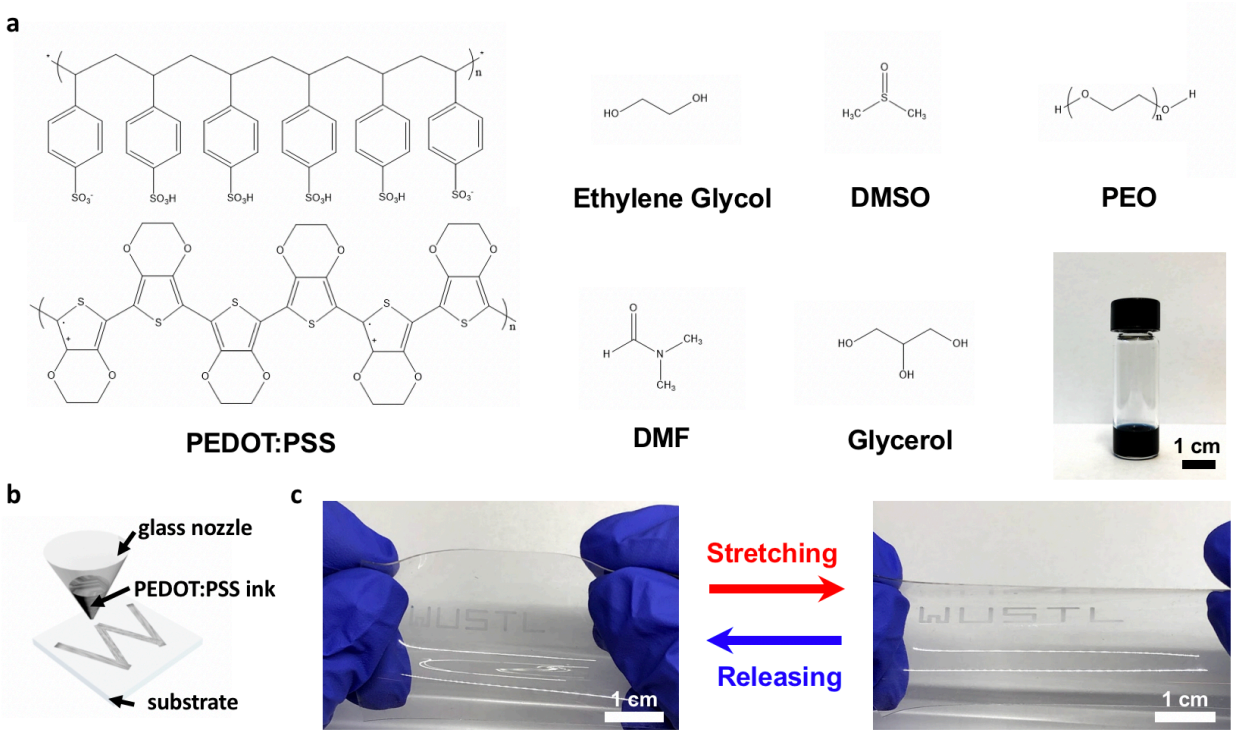

Figure 1. a) Chemical structure of the conducting polymer PEDOT:PSS, the solvent EG, DMSO, DMF, glycerol, the soft polymer PEO and a photo of the optimized ink solution containing composite of PEDOT:PSS, ethylene glycol and PEO**.** b) Schematic diagram showing the inkjet printing process on elastomer substrate. c) Photos showing a PDMS substrate with 5 layers of printed patterns of the conducting polymer in relaxed and stretched states.

Figure 2.

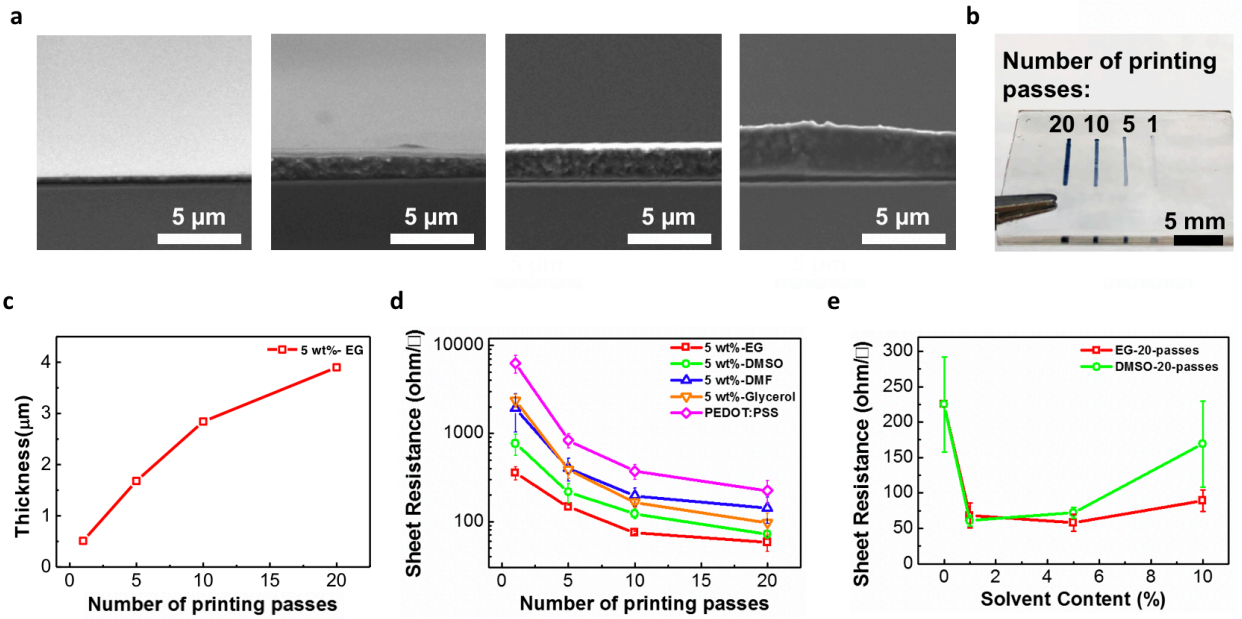

Figure 2. a) SEM images showing the thickness of inkjet-printed PEDOT:PSS thin film with 5 wt% EG after 1, 5, 10 and 20 print pass(es) (from left to right) respectively. b) Photograph of inkjet-printed PEDOT:PSS thin film on PDMS with various numbers of print passes. c) Thickness of the inkjet-printed PEDOT:PSS thin film with 5 wt% EG versus the number of print passes. d) Comparison of the sheet resistance between the pristine PEDOT:PSS ink and PEDOT:PSS mixed with 5 wt% of various types of polar solvent additives after various numbers of print passes. e) Comparison between the sheet resistance of PEDOT:PSS thin film with EG or DMSO additives with various amount of polar solvent content from 0%, 1%, 5% to 10%.

Figure 3.

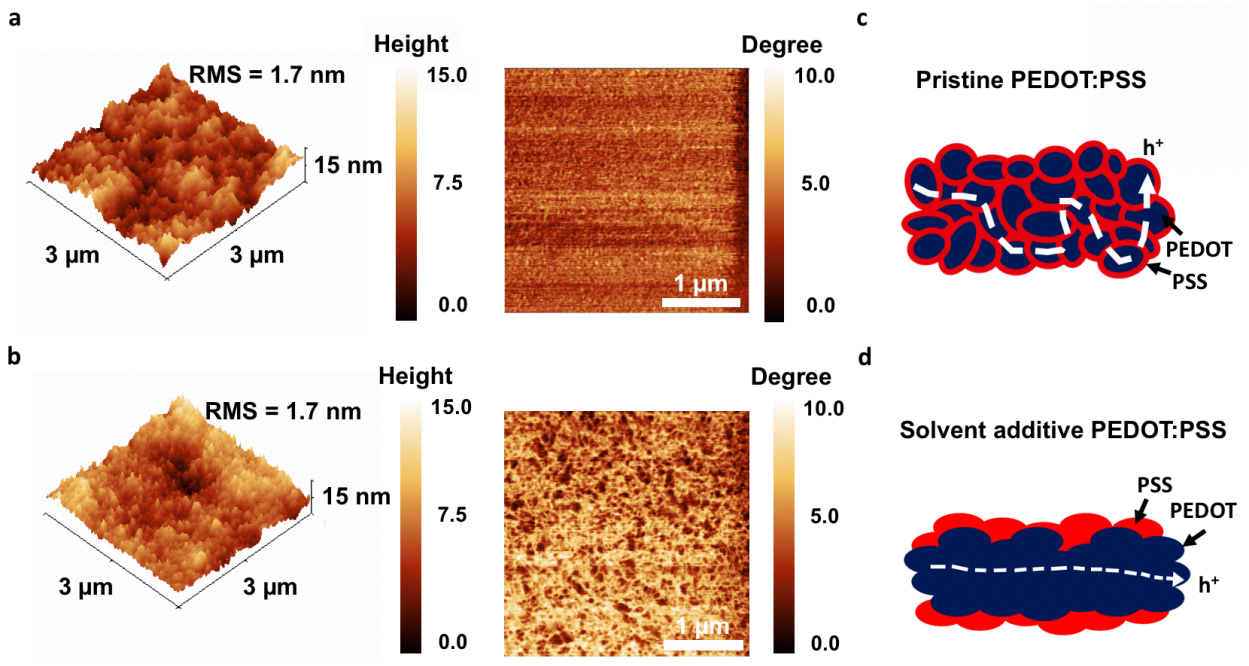

Figure 3. Morphology of the pristine PEDOT:PSS thin film and PEDOT:PSS thin film with 5 wt% EG. Height and phase images of printed thin films of a) PEDOT:PSS and b) PEDOT:PSS with 5 wt% EG obtained with tapping-mode AFM. c) Schematic illustration of the hole transport in pristine PEDOT:PSS thin film. d) Schematic illustrating the PEDOT:PSS phase separation and structural rearrangement after addition of EG.

Figure 4.

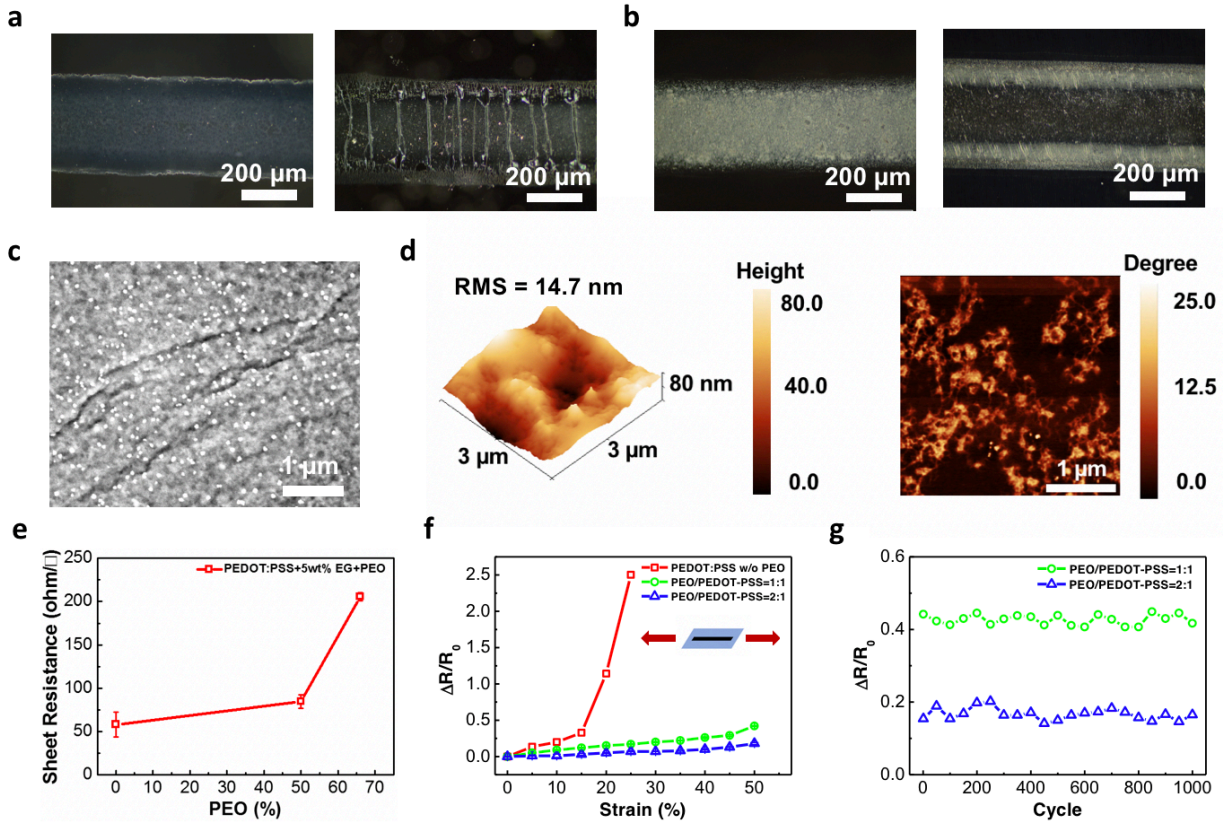

Figure 4. a) Optical micrographs of printed thin films of PEDOT:PSS with 5 wt% EG under 0% (left) and 50% (right) of tensile strain, showing the propagation of microcracks and structural failure when the film is stretched. b) Optical micrographs of printed thin films of PEDOT:PSS with 5 wt% EG and 66 wt % of PEO under 0% (left) and 50% (right) of tensile strain, indicating significantly less cracks appear in the thin film. c) SEM image showing the microstructure of the PEDOT:PSS thin film with 5 wt% EG and 66 wt% of PEO. d) Tapping mode AFM height and phase images showing the surface morphology of the PEDOT:PSS thin film with 5 wt% EG and 66 wt% of PEO. e) Sheet resistance of the inkjet-printed PEDOT:PSS thin film with 5 wt% EG and various amount of PEO. f) Relative change in resistance plotted as a function of tensile strain for PEDOT:PSS thin film with 5 wt% EG and various amount of PEO. g) Electrical property of the PEDOT:PSS/PEO film under cyclic stretching test with 50% tensile strain.

Figure 5.

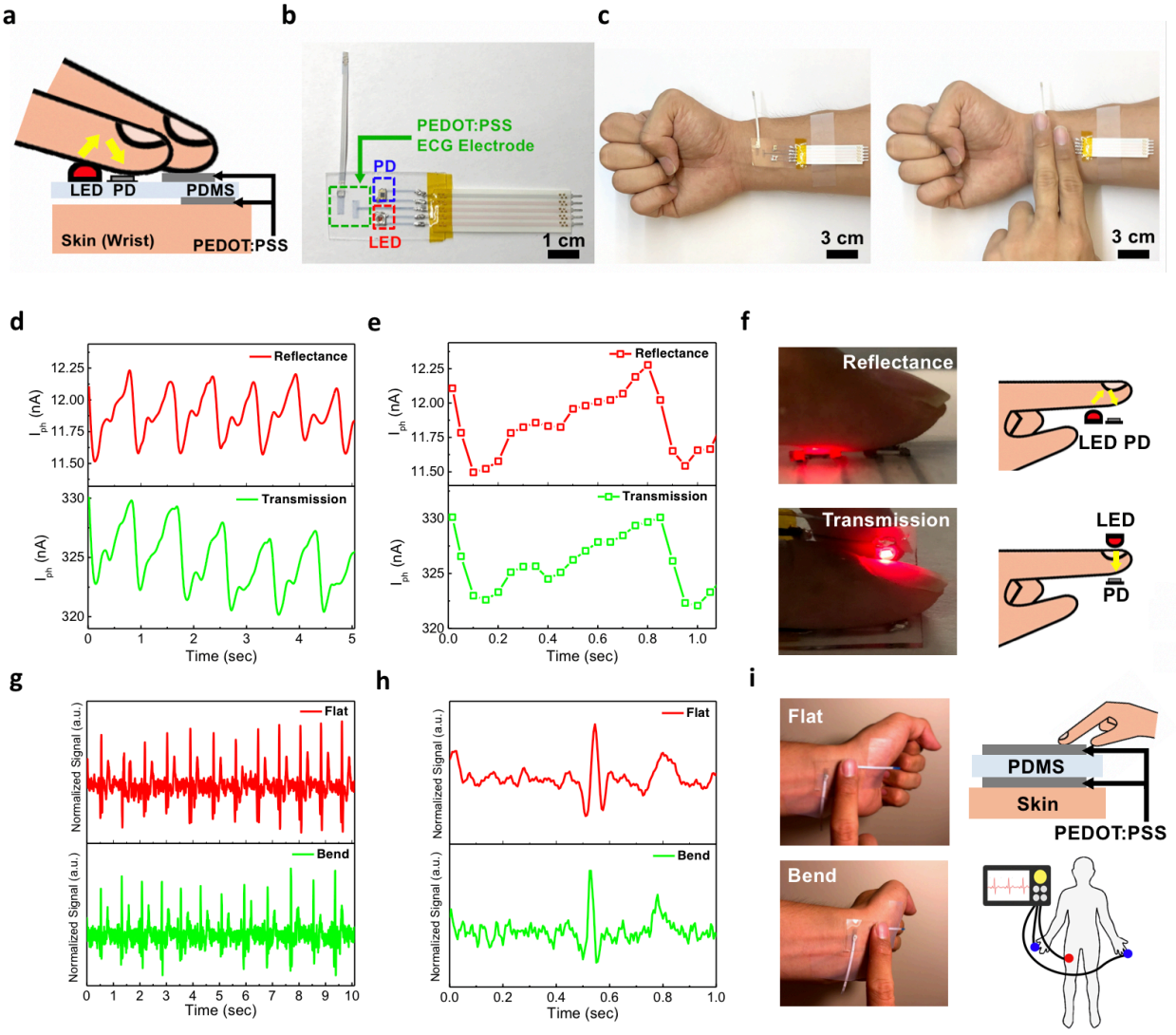

Figure 5. Representative applications of the printed stretchable PEDOT:PSS/PEO conductor for wearable electrocardiography (ECG) and photoplethysmography (PPG) sensors. a) Schematic diagram of a PDMS patch with integrated ECG and PPG sensors for simultaneous recording of both physiological signals. b) Photograph of the sensor patch with integrated ECG and PPG sensors. c) Photograph showing the placement of sensor patch on a human body for ECG and PPG recording. d, e) PPG waveforms measured with 625 nm LED illumination using both reflective and transmission mode. f) Photographs showing the experimental setup for reflectance and transmission mode PPG measurement. g, h) ECG signals measured with printed PEDOT:PSS/EG/PEO electrodes. i) Photographs and schematics showing the ECG electrode placement on the skin surface during the ECG measurements.

REFERNECES

(1) Bi, C.; Chen, B.; Wei, H.; DeLuca, S.; Huang, J. Efficient Flexible Solar Cell Based on Composition-Tailored Hybrid Perovskite. *Adv. Mater.* **2017**, *29*, 1605900.

(2) Takei, K.; Honda, W.; Harada, S.; Arie, T.; Akita, S. Toward Flexible and Wearable Human-Interactive Health-Monitoring Devices. *Adv. Healthc. Mater.* **2015**, *4*, 487–500.

(3) Khan, Y.; Han, D.; Pierre, A.; Ting, J.; Wang, X.; Lochner, C. M.; Bovo, G.; Yaacobi-Gross, N.; Newsome, C.; Wilson, R.; Arias, A. C. A Flexible Organic Reflectance Oximeter Array. *Proc. Natl. Acad. Sci. U. S. A.* **2018**, *115*, E11015–E11024.

(4) Choi, M.; Park, Y. J.; Sharma, B. K.; Bae, S. R.; Kim, S. Y.; Ahn, J. H. Flexible Active-Matrix Organic Light-Emitting Diode Display Enabled by MoS2 Thin-Film Transistor. *Sci. Adv.* **2018**, *4*, eaas8721.

(5) Gao, W.; Emaminejad, S.; Nyein, H. Y. Y.; Challa, S.; Chen, K.; Peck, A.; Fahad, H. M.; Ota, H.; Shiraki, H.; Kiriya, D.; Lien, D. H.; Brooks, G. A.; Davis, R. W.; Javey, A. Fully Integrated Wearable Sensor Arrays for Multiplexed in Situ Perspiration Analysis. *Nature* **2016**, *529*, 509–514.

(6) Yu, M.; Wan, H.; Cai, L.; Miao, J.; Zhang, S.; Wang, C. Fully Printed Flexible Dual-Gate Carbon Nanotube Thin-Film Transistors with Tunable Ambipolar Characteristics for Complementary Logic Circuits. *ACS Nano* **2018**, *12*, 11572–11578.

(7) Wan, H.; Cao, Y.; Lo, L.; Zhao, J.; Sepúlveda, N.; Wang, C. Flexible Carbon Nanotube Synaptic Transistor for Neurological Electronic Skin Applications. *ACS Nano* **2020**, *14*, 10402–10412.

(8) Rao, Z.; Ershad, F.; Almasri, A.; Gonzalez, L.; Wu, X.; Yu, C. Soft Electronics for the Skin: From Health Monitors to Human–Machine Interfaces. *Adv. Mater. Technol.* **2020**, *5*, 2000233.

(9) Jeong, Y. R.; Kim, J.; Xie, Z.; Xue, Y.; Won, S. M.; Lee, G.; Jin, S. W.; Hong, S. Y.; Feng, X.; Huang, Y.; Rogers, J. A.; Ha, J. S. A Skin-Attachable, Stretchable Integrated System Based on Liquid GaInSn for Wireless Human Motion Monitoring with Multi-Site Sensing Capabilities. *NPG Asia Mater.* **2017**, *9*, e443.

(10) Chortos, A.; Bao, Z. Skin-Inspired Electronic Devices. *Mater. Today* **2014**, *17*, 321–331.

(11) Honda, W.; Harada, S.; Arie, T.; Akita, S.; Takei, K. Wearable, Human-Interactive, Health-Monitoring, Wireless Devices Fabricated by Macroscale Printing Techniques. *Adv. Funct. Mater.* **2014**, *24*, 3299–3304.

(12) Yamamoto, Y.; Yamamoto, D.; Takada, M.; Naito, H.; Arie, T.; Akita, S.; Takei, K. Efficient Skin Temperature Sensor and Stable Gel-Less Sticky ECG Sensor for a Wearable Flexible Healthcare Patch. *Adv. Healthc. Mater.* **2017**, *6*, 1700495.

(13) Zhang, S.; Cai, L.; Li, W.; Miao, J.; Wang, T.; Yeom, J.; Sepúlveda, N.; Wang, C. Fully Printed Silver-Nanoparticle-Based Strain Gauges with Record High Sensitivity. *Adv. Electron. Mater.* **2017**, *3*, 1700067.

(14) Cotur, Y.; Kasimatis, M.; Kaisti, M.; Olenik, S.; Georgiou, C.; Güder, F. Stretchable Composite Acoustic Transducer for Wearable Monitoring of Vital Signs. *Adv. Funct. Mater.* **2020**, *30*, 1910288.

(15) Cai, L.; Zhang, S.; Zhang, Y.; Li, J.; Miao, J.; Wang, Q.; Yu, Z.; Wang, C. Direct Printing for Additive Patterning of Silver Nanowires for Stretchable Sensor and Display Applications. *Adv. Mater. Technol.* **2018**, *3*, 1700232.

(16) Bade, S. G. R.; Shan, X.; Hoang, P. T.; Li, J.; Geske, T.; Cai, L.; Pei, Q.; Wang, C.; Yu, Z. Stretchable Light-Emitting Diodes with Organometal-Halide-Perovskite–Polymer Composite Emitters. *Adv. Mater.* **2017**, *29*, 1607053.

(17) Pu, X.; Liu, M.; Chen, X.; Sun, J.; Du, C.; Zhang, Y.; Zhai, J.; Hu, W.; Wang, Z. L. Ultrastretchable, Transparent Triboelectric Nanogenerator as Electronic Skin for Biomechanical Energy Harvesting and Tactile Sensing. *Sci. Adv.* **2017**, *3*, e1700015.

(18) Rogers, J. A.; Someya, T.; Huang, Y. Materials and Mechanics for Stretchable Electronics. *Science.* **2010**, *327*, 1603–1607.

(19) Lo, L. W.; Shi, H.; Wan, H.; Xu, Z.; Tan, X.; Wang, C. Inkjet-Printed Soft Resistive Pressure Sensor Patch for Wearable Electronics Applications. *Adv. Mater. Technol.* **2020**, *5*, 1900717.

(20) Shi, H.; Al-Rubaiai, M.; Holbrook, C. M.; Miao, J.; Pinto, T.; Wang, C.; Tan, X. Screen-Printed Soft Capacitive Sensors for Spatial Mapping of Both Positive and Negative Pressures. *Adv. Funct. Mater.* **2019**, *29*, 1809116.

(21) Tang, J.; Guo, H.; Zhao, M.; Yang, J.; Tsoukalas, D.; Zhang, B.; Liu, J.; Xue, C.; Zhang, W. Highly Stretchable Electrodes on Wrinkled Polydimethylsiloxane Substrates. *Sci. Rep.* **2015**, *5*, 16527.

(22) Khang, D. Y.; Rogers, J. A.; Lee, H. H. Mechanical Buckling: Mechanics, Metrology, and Stretchable Electronics. *Adv. Funct. Mater.* **2009**, *19*, 1526–1536.

(23) Sun, Y.; Kumar, V.; Adesida, I.; Rogers, J. A. Buckled and Wavy Ribbons of GaAs for High-Performance Electronics on Elastomeric Substrates. *Adv. Mater.* **2006**, *18*, 2857–2862.

(24) Kim, T.; Park, J.; Sohn, J.; Cho, D.; Jeon, S. Bioinspired, Highly Stretchable, and Conductive Dry Adhesives Based on 1D-2D Hybrid Carbon Nanocomposites for All-in-One ECG Electrodes. *ACS Nano* **2016**, *10*, 4770–4778.

(25) Oh, J. Y.; Jun, G. H.; Jin, S.; Ryu, H. J.; Hong, S. H. Enhanced Electrical Networks of

Stretchable Conductors with Small Fraction of Carbon Nanotube/Graphene Hybrid Fillers. *ACS Appl. Mater. Interfaces* **2016**, *8*, 3319–3325.

(26) Larmagnac, A.; Eggenberger, S.; Janossy, H.; Vörös, J. Stretchable Electronics Based on Ag-PDMS Composites. *Sci. Rep.* **2014**, *4*, 7254.

(27) Kim, Y.; Zhu, J.; Yeom, B.; Di Prima, M.; Su, X.; Kim, J. G.; Yoo, S. J.; Uher, C.; Kotov, N. A. Stretchable Nanoparticle Conductors with Self-Organized Conductive Pathways. *Nature* **2013**, *500*, 59–63.

(28) Hu, W.; Niu, X.; Li, L.; Yun, S.; Yu, Z.; Pei, Q. Intrinsically Stretchable Transparent Electrodes Based on Silver-Nanowire-Crosslinked-Polyacrylate Composites. *Nanotechnology* **2012**, *23*, 344002.

(29) Chen, Y.; Carmichael, R. S.; Carmichael, T. B. Patterned, Flexible, and Stretchable Silver Nanowire/Polymer Composite Films As Transparent Conductive Electrodes. *ACS Appl. Mater. Interfaces* **2019**, *11*, 31210–31219.

(30) Tseng, Y. T.; Lin, Y. C.; Shih, C. C.; Shih, C. C.; Hsieh, H. C.; Lee, W. Y.; Chiu, Y. C.; Chen, W. C.; Chen, W. C. Morphology and Properties of PEDOT:PSS/Soft Polymer Blends through Hydrogen Bonding Interaction and Their Pressure Sensor Application. *J. Mater. Chem. C* **2020**, *8*, 6013–6024.

(31) Dauzon, E.; Lin, Y.; Faber, H.; Yengel, E.; Sallenave, X.; Plesse, C.; Goubard, F.; Amassian, A.; Anthopoulos, T. D. Stretchable and Transparent Conductive PEDOT:PSS-Based Electrodes for Organic Photovoltaics and Strain Sensors Applications. *Adv. Funct. Mater.* **2020**, *30*, 2001251.

(32) Lee, J. H.; Jeong, Y. R.; Lee, G.; Jin, S. W.; Lee, Y. H.; Hong, S. Y.; Park, H.; Kim, J. W.; Lee, S. S.; Ha, J. S. Highly Conductive, Stretchable, and Transparent PEDOT:PSS

Electrodes Fabricated with Triblock Copolymer Additives and Acid Treatment. *ACS Appl. Mater. Interfaces* **2018**, *10*, 28027–28035.

(33) Li, P.; Sun, K.; Ouyang, J. Stretchable and Conductive Polymer Films Prepared by Solution Blending. *ACS Appl. Mater. Interfaces* **2015**, *7*, 18415–18423.

(34) Choong, C. L.; Shim, M. B.; Lee, B. S.; Jeon, S.; Ko, D. S.; Kang, T. H.; Bae, J.; Lee, S. H.; Byun, K. E.; Im, J.; Jeong, Y. J.; Park, C. E.; Park, J. J.; Chung, U. I. Highly Stretchable Resistive Pressure Sensors Using a Conductive Elastomeric Composite on a Micropyramid Array. *Adv. Mater.* **2014**, *26*, 3451–3458.

(35) Vosgueritchian, M.; Lipomi, D. J.; Bao, Z. Highly Conductive and Transparent PEDOT:PSS Films with a Fluorosurfactant for Stretchable and Flexible Transparent Electrodes. *Adv. Funct. Mater.* **2012**, *22*, 421–428.

(36) Lipomi, D. J.; Lee, J. A.; Vosgueritchian, M.; Tee, B. C.; Bolander, J. A. On Stretchable Substrates. *Chem. Mater.* **2012**, *24*, 373.

(37) Jung, S.; Sou, A.; Gili, E.; Sirringhaus, H. Inkjet-Printed Resistors with a Wide Resistance Range for Printed Read-Only Memory Applications. *Org. Electron.* **2013**, *14*, 699–702.

(38) Hoath, S. D.; Hsiao, W. K.; Martin, G. D.; Jung, S.; Butler, S. A.; Morrison, N. F.; Harlen, O. G.; Yang, L. S.; Bain, C. D.; Hutchings, I. M. Oscillations of Aqueous PEDOT:PSS Fluid Droplets and the Properties of Complex Fluids in Drop-on-Demand Inkjet Printing. *J. Nonnewton. Fluid Mech.* **2015**, *223*, 28–36.

(39) Basak, I.; Nowicki, G.; Ruttens, B.; Desta, D.; Prooth, J.; Jose, M.; Nagels, S.; Boyen, H. G.; D'haen, J.; Buntinx, M.; Deferme, W. Inkjet Printing of PEDOT:PSS Based Conductive Patterns for 3D Forming Applications. *Polymers* **2020**, *12*, 2915.

(40) Li, L.; Pan, L.; Ma, Z.; Yan, K.; Cheng, W.; Shi, Y.; Yu, G. All Inkjet-Printed

Amperometric Multiplexed Biosensors Based on Nanostructured Conductive Hydrogel Electrodes. *Nano Lett.* **2018**, *18*, 3322–3327.

(41) Huang, T. T.; Wu, W. Inkjet-Printed Wearable Nanosystems for Self-Powered Technologies. *Adv. Mater. Interfaces* **2020**, *7*, 2000015.

(42) Sico, G.; Montanino, M.; De Girolamo Del Mauro, A.; Minarini, C. Improving the Gravure Printed PEDOT:PSS Electrode by Gravure Printing DMSO Post-Treatment. *J. Mater. Sci. Mater. Electron.* **2018**, *29*, 11730–11737.

(43) Sico, G.; Montanino, M.; De Girolamo Del Mauro, A.; Imparato, A.; Nobile, G.; Minarini, C. Effects of the Ink Concentration on Multi-Layer Gravure-Printed PEDOT:PSS. *Org. Electron.* **2016**, *28*, 257–262.

(44) Fan, X.; Nie, W.; Tsai, H.; Wang, N.; Huang, H.; Cheng, Y.; Wen, R.; Ma, L.; Yan, F.; Xia, Y. PEDOT:PSS for Flexible and Stretchable Electronics: Modifications, Strategies, and Applications. *Adv. Sci.* **2019**, *6*, 1900813.

(45) Carrasco-Torres, G.; Valdés-Madrigal, M. A.; Vásquez-Garzón, V. R.; Baltiérrez-Hoyos, R.; De la Cruz-Burelo, E. D.; Román-Doval, R.; Valencia-Lazcano, A. A. Effect of Silk Fibroin on Cell Viability in Electrospun Scaffolds of Polyethylene Oxide. *Polymers* **2019**, *11*, 451.

(46) Vomero, M.; Castagnola, E.; Ciarpella, F.; Maggiolini, E.; Goshi, N.; Zucchini, E.; Carli, S.; Fadiga, L.; Kassegne, S.; Ricci, D. Highly Stable Glassy Carbon Interfaces for Long-Term Neural Stimulation and Low-Noise Recording of Brain Activity. *Sci. Rep.* **2017**, *7*, 40332.

(47) Jabbar, F.; Soomro, A. M.; Lee, J. W.; Ali, M.; Su Kim, Y.; Lee, S. H.; Choi, K. H. Robust Fluidic Biocompatible Strain Sensor Based on PEDOT:PSS/CNT Composite for

Human-Wearable and High-End Robotic Applications. *Sensors Mater.* **2020**, *32*, 4077–4093.

(48) Monteiro A., I.; Kollmetz, T.; Musson, D. S.; McGlashan, S. R.; Malmström, J. Polystyrene- Block -Polyethylene Oxide Thin Films: In Vitro Cytocompatibility and Protein Adsorption Testing . *Biointerphases* **2020**, *15*, 011003.

(49) Ouyang, J.; Xu, Q.; Chu, C. W.; Yang, Y.; Li, G.; Shinar, J. On the Mechanism of Conductivity Enhancement in Poly(3,4- Ethylenedioxythiophene):Poly(Styrene Sulfonate) Film through Solvent Treatment. *Polymer* **2004**, *45*, 8443.

(50) Wijeratne, K.; Ail, U.; Brooke, R.; Vagin, M.; Liu, X.; Fahlman, M.; Crispin, X. Bulk Electronic Transport Impacts on Electron Transfer at Conducting Polymer Electrode–Electrolyte Interfaces. *Proc. Natl. Acad. Sci. U. S. A.* **2018**, *115*, 11899.

(51) Wang, Y.; Song, R.; Li, Y.; Shen, J. Understanding Tapping-Mode Atomic Force Microscopy Data on the Surface of Soft Block Copolymers. *Surf. Sci.* **2003**, *530*, 136–148.

(52) Kayser, L. V.; Lipomi, D. J. Stretchable Conductive Polymers and Composites Based on PEDOT and PEDOT:PSS. *Adv. Mater.* **2019**, *31*, 1806133.

(53) Luo, R.; Li, H.; Du, B.; Zhou, S.; Zhu, Y. A Simple Strategy for High Stretchable, Flexible and Conductive Polymer Films Based on PEDOT:PSS-PDMS Blends. *Org. Electron.* **2020**, *76*, 105451.

(54) Taroni, P. J.; Santagiuliana, G.; Wan, K.; Calado, P.; Qiu, M.; Zhang, H.; Pugno, N. M.; Palma, M.; Stingelin-Stutzman, N.; Heeney, M.; Fenwick, O.; Baxendale, M.; Bilotti, E. Toward Stretchable Self-Powered Sensors Based on the Thermoelectric Response of PEDOT:PSS/Polyurethane Blends. *Adv. Funct. Mater.* **2018**, *28*, 1704285.

(55) Ratna, D.; Divekar, S.; Samui, A. B.; Chakraborty, B. C.; Banthia, A. K. Poly(Ethylene Oxide)/Clay Nanocomposite: Thermomechanical Properties and Morphology. *Polymer* **2006**, *47*, 4068–4074.

(56) Wang, T.; Qi, Y.; Xu, J.; Hu, X.; Chen, P. Effects of Poly(Ethylene Glycol) on Electrical Conductivity of Poly(3,4-Ethylenedioxythiophene)-Poly(Styrenesulfonic Acid) Film. *Appl. Surf. Sci.* **2005**, *250*, 188–194.

(57) Yuk, H.; Lu, B.; Zhao, X. Hydrogel Bioelectronics. *Chem. Soc. Rev.* **2019**, *48*, 1642–1667.

(58) Tamura, T.; Maeda, Y.; Sekine, M.; Yoshida, M. Wearable Photoplethysmographic Sensors—Past and Present. *Electron.* **2014**, *3*, 282–302.

(59) Klabunde, R. E. Cardiac Electrophysiology: Normal and Ischemic Ionic Currents and the ECG. *Adv. Physiol. Educ.* **2017**, *41*, 29–37.

(60) Luz, E. J. da S.; Schwartz, W. R.; Cámara-Chávez, G.; Menotti, D. ECG-Based Heartbeat Classification for Arrhythmia Detection: A Survey. *Comput. Methods Programs Biomed.* **2016**, *127*, 144–164.

(61) Birnbaum, Y.; Drew, B. J. The Electrocardiogram in ST Elevation Acute Myocardial Infarction: Correlation with Coronary Anatomy and Prognosis. *Postgrad. Med. J.* **2003**, *79*, 490–504.

TOC Figure

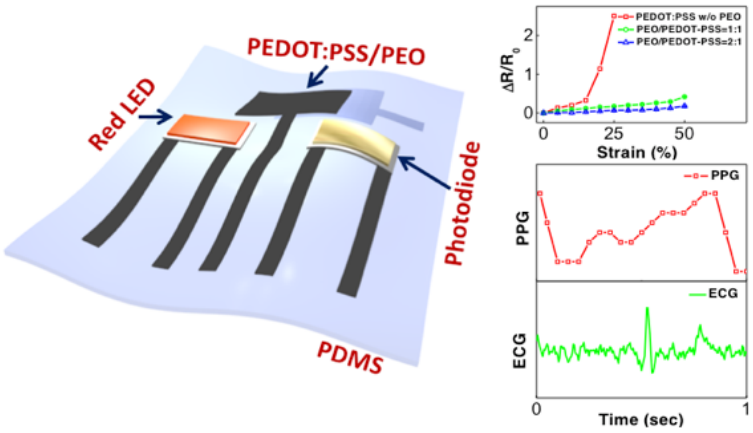
PEDOT:PSS/PEO
Red LED
Photodiode
PDMS
PEDOT:PSS w/o PEO
PEO/PEDOT-PSS=1:1
PEO/PEDOT-PSS=2:1
ΔR/R0
Strain (%)
PPG
ECG
Time (sec)

Supporting Information

Inkjet-Printed PEDOT:PSS-based Stretchable Conductor for Wearable Health Monitoring Device Applications

Li-Wei Lo,[†,§] Junyi Zhao,[†] Haochuan Wan,[†] Yong Wang,[†,‡] Shantanu Chakrabartty,[†] and Chuan Wang[,†,§]*

[†] Department of Electrical & Systems Engineering, Washington University in St. Louis, St. Louis, Missouri 63130, United States

[§] Institute of Materials Science and Engineering, Washington University in St. Louis, St. Louis, Missouri 63130, United States

[‡] Department of Obstetrics & Gynecology, Washington University in St. Louis, St. Louis, Missouri 63130, United States

[*] Corresponding author: chuanwang@wustl.edu

S1. UV-Vis spectra of inkjet-printed PEDOT:PSS thin film

Figure S1 presents the UV-vis spectra of inkjet-printed PEDOT:PSS thin film with 5, 10 and 20 print passes. The spectra show the transmittance decreases gradually for increasing number of printing passes. The result agree with the photo in Figure 2b where the PEDOT:PSS pattern with 20 print passes is the least transparent.

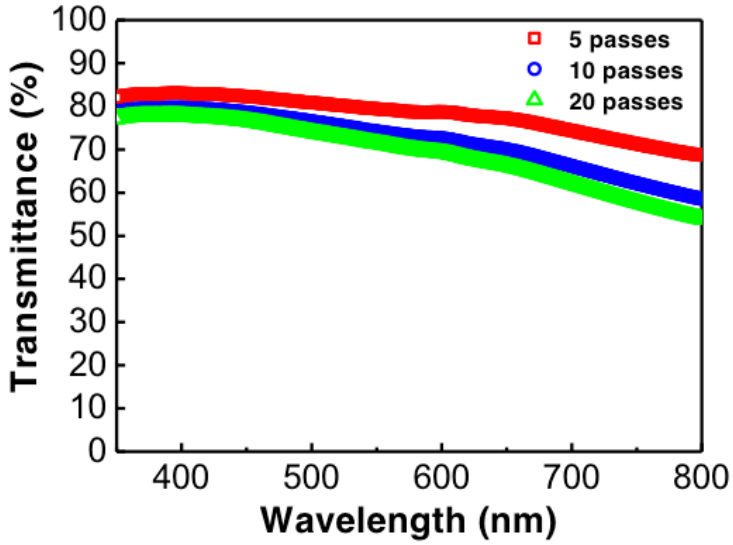

Figure S1. UV-Vis spectra of printed PEDOT:PSS thin film with different numbers of printing passes.

S2. Electrical characterization of the printed PEDOT:PSS/PEO thin film over time

Figure S2 shows the sheet resistance of inkjet-printed PEDOT:PSS thin film with 5 wt% EG and various amount of PEO measured again after 1.5 months. Due to the hygroscopic nature of PSS that absorbs moisture from surrounding environment, the sheet resistance of the PEDOT:PSS/PEO thin film gradually increases over time. The red trace was the data measured right after the thin film was fabricated and the blue trace shows the sheet resistance of the same sample after 1.5 months. The sheet resistance increased from 58 Ω/□ to 91 Ω/□, 84 Ω/□ to 131 Ω/□, and 205 Ω/□ to 317 Ω/□, for printed thin films of pristine PEDOT:PSS, and PEDOT:PSS with 50 wt% and 66 wt% of PEO, respectively.

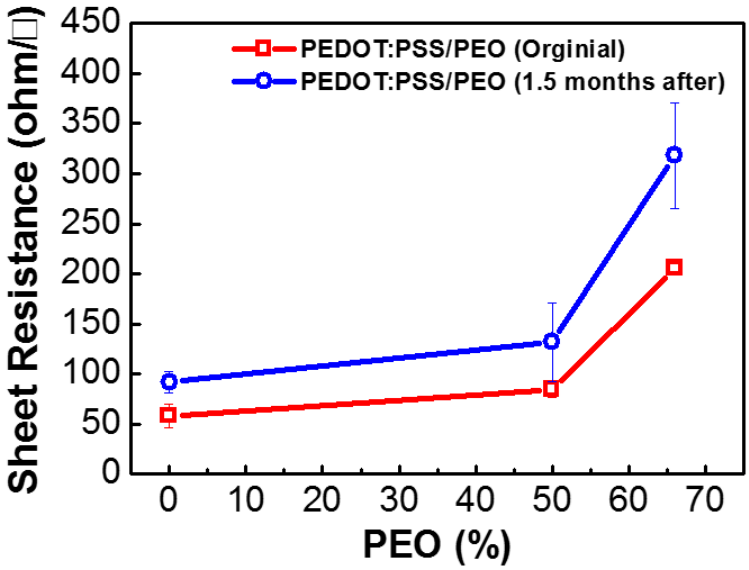

Figure S2. Comparison of sheet resistance of inkjet-printed PEDOT:PSS thin film with 5wt% EG and various amount of PEO measured again after 1.5 months.

S3. Electrical Properties of PEDOT:PSS/PEO thin film when stretched along the transverse direction

Figure S3 shows the relative change in resistance plotted as a function of tensile strain for PEDOT:PSS thin film with 5 wt% EG and various amount of PEO when stretched along the transverse direction. In this experiment, the printed pattern is a straight line with ~ 450 μm width and ~1.5 cm length. For the results presented in Figure 4f, when stretched along the longitudinal direction by 50%, the devices experience 41% and 18% increase in sheet resistance for samples with 50 wt% and 66 wt% of PEO additives, respectively. When stretched along the transverse direction, the samples exhibit 61% and 32% increase in sheet resistance for samples with 50 wt% and 66 wt% of PEO additives, respectively. The increase in sheet resistance may be because the PEDOT grains tend to be stacked along the printing direction (longitudinal direction) during printing. As a result, the stretching in the transverse direction may have more impact on the grains sliding than stretching along the printing direction.

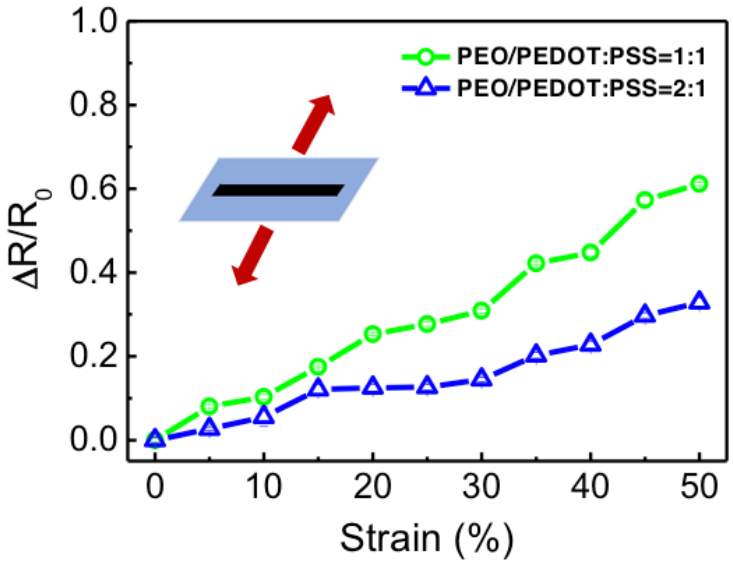

Figure S3. Relatively change in resistance as a function of tensile strain when the sample is stretched along the transverse direction.

S4. Rheological properties of the PEDOT:PSS-based conducting polymer ink

Figure S4 shows the viscosity as a function of shear rate for the PEDOT:PSS-based conducting polymer inks with various types of additives. The viscosity was measured (Rheometer, TA Instruments AR G2) at the shear rate from 1 to 1000 s^{-1}. The results show typical non-Newtonian behavior of the PEDOT:PSS solution with decreasing viscosity for increasing shear rates.[1,2] For the pristine PEDOT:PSS ink, the viscosity is 0.1863 Pa-s at a shear rate 1 s^{-1} and the viscosity drop to 0.02327 Pa-s at a shear rate 1000 s^{-1}. The PEDOT:PSS solution mixed with 5wt% of EG, DMSO DMF and glycerol all exhibit similar behavior compare with pristine PEDOT:PSS ink. Moreover, the PEDOT:PSS mixed with 5 wt% EG and 50 wt% PEO (PEO/PEDOT:PSS = 1:1) or 5 wt% EG and 66 wt% PEO (PEO/PEDOT:PSS = 2:1) exhibit higher viscosity compared to the one without PEO under all shear rates tested. The result may be attributed to the high molecular weight of PEO. At a shear rate of 1000 s-1, the viscosity of the PEO/PEDOT:PSS mixture exhibit a fairly low viscosity of 0.041 and 0.039 Pa-s for 50 wt% of PEO and 66 wt% of PEO, respectively. Our ink exhibit similar rheological behavior compared to the viscosity of PEDOT:PSS solution reported previously in the literature.[3,4]

Typically, the inkjet printer has a shear rate greater than 1000 s^{-1} and the printability of the ink is defined by the Ohnesorge number whose value typically lies between 0.1 to 10.[5–8] In supporting information Table S2, we have systematically measured and provided the detailed information about the ink properties including the ink density, surface tension and the calculated Ohnesorge number. The inkjet printer used in this experiment (The GIX Microplotter, Sonoplot Inc.) is capable of printing inks with viscosity up to 0.450 Pa-s and the calculated Ohnesorge number for all types of PEDOT:PSS solution fall in the range between 0.1 to 10. Therefore, all types of PEDOT:PSS solution in this work are printable by inkjet printing process.

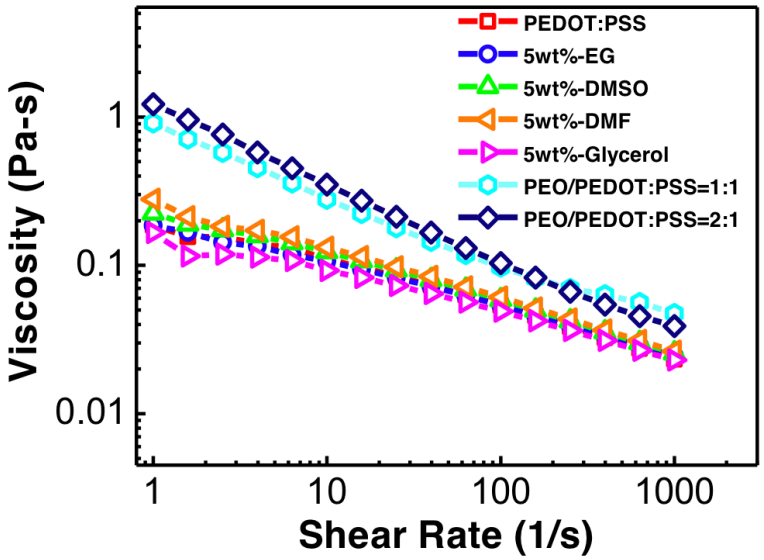

Figure S4. Measured viscosity as a function of shear rate for the PEDOT:PSS-based conducting polymer inks with various types of additives.

Table S1. Comparison of PEDOT:PSS based conductor with various kinds of treatment and fabrication methods

Materials	Fabrication Method	Stretchability	Conductivity / Sheet resistance
PEDOT:PSS with H_2SO_4 post-treatment [9]	spin-cast	N/A	4380 S cm^{-1}
PEDOT:PSS hydrogel with H_2SO_4 treatment [10]	blade cast	N/A	880 S cm^{-1}
H_2SO_4/DMSO-treated PEDOT:PSS [11]	spin coating with layer-by-layer (LBL) process	N/A	3026 S cm^{-1}
PEDOT:PSS doped with benzenesulfonic acid [12]	spin coating	N/A	1996 S cm^{-1}
PEDOT:PSS with H_2SO_4 treatment [13]	spin-cast	N/A	2938 S cm^{-1}
PEDOT:PSS with PEG and EG [14]	spin coating	~ 25%	101 S cm^{-1}
PEDOT:PSS with PVA and EG [14]	spin coating	47%	172 S cm^{-1}
PEDOT:PSS with PDMS EG and Triton-X 100 [15]	molding	82%	20 Ω/□
PEDOT:PSS with poly(acrylic acid) (PAA) [16]	spin coating	40%	125 S cm^{-1}
PEDOT:PSS with PU [17]	drop cast	700%	79 S cm^{-1}

Table S2. Summary of ink formulations and measured properties

Ink Composition	Density (kg/m^3)	Surface Tension (J/m^2)	Nozzle Diameter (m)	Viscosity (Pa-s) at shear rate = 1000 (1/s)	Ohnesorge Nummer
PEDOT:PSS	1020.00	0.0725	0.0004	0.02327	0.135
PEDOT:PSS + 5wt% EG	1040.00	0.0706	0.0004	0.02456	0.143
PEDOT:PSS + 5wt% DMSO	1065.33	0.0687	0.0004	0.0256	0.149
PEDOT:PSS + 5wt% DMF	1002.67	0.0653	0.0004	0.02636	0.162
PEDOT:PSS + 5wt% Glycerol	1091.67	0.0760	0.0004	0.02294	0.125
PEO/PEDOT:PSS = 1:1	1012.00	0.0540	0.0004	0.04736	0.320
PEO/PEDOT:PSS = 2:1	1030.38	0.0543	0.0004	0.03894	0.260

Supplementary References

(1) Basak, I.; Nowicki, G.; Ruttens, B.; Desta, D.; Prooth, J.; Jose, M.; Nagels, S.; Boyen, H. G.; D'haen, J.; Buntinx, M.; Deferme, W. Inkjet Printing of PEDOT:PSS Based Conductive Patterns for 3D Forming Applications. *Polymer.* **2020**, *12*, 2915.

(2) Yuk, H.; Lu, B.; Lin, S.; Qu, K.; Xu, J.; Luo, J.; Zhao, X. 3D Printing of Conducting Polymers. *Nat. Commun.* **2020**, *11*, 1604.

(3) Hoath, S. D.; Jung, S.; Hsiao, W. K.; Hutchings, I. M. How PEDOT:PSS Solutions Produce Satellite-Free Inkjets. *Org. Electron.* **2012**, *13*, 3259–3262.

(4) Gemeiner, P.; Peřinka, N.; Švorc, Ľ.; Hatala, M.; Gál, L.; Belovičová, M.; Syrový, T.; Mikula, M. Pt–Free Counter Electrodes Based on Modified Screen–Printed PEDOT:PSS Catalytic Layers for Dye–Sensitized Solar Cells. *Mater. Sci. Semicond. Process.* **2017**, *66*, 162–169.

(5) Van Driessche, I.; Feys, J.; Hopkins, S. C.; Lommens, P.; Granados, X.; Glowacki, B. A.; Ricart, S.; Holzapfel, B.; Vilardell, M.; Kirchner, A.; Bäcker, M. Chemical Solution Deposition Using Ink-Jet Printing for YBCO Coated Conductors. *Supercond. Sci. Technol.* **2012**, *25*, 065017.

(6) Derby, B. Inkjet Printing of Functional and Structural Materials: Fluid Property Requirements, Feature Stability, and Resolution. *Annu. Rev. Mater. Res.* **2010**, *40*, 395–414.

(7) Yang, L.; Kazmierski, B. K.; Hoath, S. D.; Jung, S.; Hsiao, W. K.; Wang, Y.; Berson, A.; Harlen, O.; Kapur, N.; Bain, C. D. Determination of Dynamic Surface Tension and Viscosity of Non-Newtonian Fluids from Drop Oscillations. *Phys. Fluids* **2014**, *26*, 113103.

(8) Dybowska-Sarapuk, L.; Kielbasinski, K.; Arazna, A.; Futera, K.; Skalski, A.; Janczak, D.; Sloma, M.; Jakubowska, M. Efficient Inkjet Printing of Graphene-Based Elements: Influence of Dispersing Agent on Ink Viscosity. *Nanomaterials* **2018**, *8*, 602.

(9) Kim, N.; Kee, S.; Lee, S. H.; Lee, B. H.; Kahng, Y. H.; Jo, Y. R.; Kim, B. J.; Lee, K. Highly Conductive PEDOT:PSS Nanofibrils Induced by Solution-Processed Crystallization. *Adv. Mater.* **2014**, *26*, 2268–2272.

(10) Yao, B.; Wang, H.; Zhou, Q.; Wu, M.; Zhang, M.; Li, C.; Shi, G. Ultrahigh-Conductivity Polymer Hydrogels with Arbitrary Structures. *Adv. Mater.* **2017**, *29*, 1700974.

(11) Kim, Y.; Kim, Y.; Kim, J. H. Highly Conductive Pedot:Pss Thin Films with Two-Dimensional Lamellar Stacked Multi-Layers. *Nanomaterials* **2020**, *10*, 2211.

(12) Wang, C.; Sun, K.; Fu, J.; Chen, R.; Li, M.; Zang, Z.; Liu, X.; Li, B.; Gong, H.; Ouyang, J. Enhancement of Conductivity and Thermoelectric Property of PEDOT:PSS via Acid Doping and Single Post-Treatment for Flexible Power Generator. *Adv. Sustain. Syst.* **2018**, *2*, 1800085.

(13) Bießmann, L.; Saxena, N.; Hohn, N.; Hossain, M. A.; Veinot, J. G. C.; Müller-Buschbaum, P. Highly Conducting, Transparent PEDOT:PSS Polymer Electrodes from Post-Treatment with Weak and Strong Acids. *Adv. Electron. Mater.* **2019**, *5*, 1800654.

(14) Li, P.; Sun, K.; Ouyang, J. Stretchable and Conductive Polymer Films Prepared by Solution Blending. *ACS Appl. Mater. Interfaces* **2015**, *7*, 18415–18423.

(15) Luo, R.; Li, H.; Du, B.; Zhou, S.; Zhu, Y. A Simple Strategy for High Stretchable, Flexible and Conductive Polymer Films Based on PEDOT:PSS-PDMS Blends. *Org. Electron.* **2020**, *76*, 105451.

(16) Tseng, Y. T.; Lin, Y. C.; Shih, C. C.; Shih, C. C.; Hsieh, H. C.; Lee, W. Y.; Chiu, Y. C.; Chen, W. C.; Chen, W. C. Morphology and Properties of PEDOT:PSS/Soft Polymer Blends through Hydrogen Bonding Interaction and Their Pressure Sensor Application. *J. Mater. Chem. C* **2020**, *8*, 6013–6024.

(17) Taroni, P. J.; Santagiuliana, G.; Wan, K.; Calado, P.; Qiu, M.; Zhang, H.; Pugno, N. M.; Palma, M.; Stingelin-Stutzman, N.; Heeney, M.; Fenwick, O.; Baxendale, M.; Bilotti, E. Toward Stretchable Self-Powered Sensors Based on the Thermoelectric Response of PEDOT:PSS/Polyurethane Blends. *Adv. Funct. Mater.* **2018**, *28*, 1704285.